Journal of Bioenergetics and Biomembranes, Vol. 27, No. 3, 1995

Relationship Between the Oxidation Potential of the Bacteriochlorophyll Dimer and Electron Transfer in Photosynthetic Reaction Centers

J. P. Allen[1] and J. C. Williams[1]

Received March 8, 1995

The primary electron donor in the photosynthetic reaction center from purple bacteria is a bacteriochlorophyll dimer containing four conjugated carbonyl groups that may form hydrogen bonds with amino acid residues. Spectroscopic analyses of a set of mutant reaction centers confirm that hydrogen bonds can be formed between each of these carbonyl groups and histidine residues in the reaction center subunits. The addition of each hydrogen bond is correlated with an increase in the oxidation potential of the dimer, resulting in a 355-mV range in the midpoint potential. The resulting changes in the free-energy differences for several reactions involving the dimer are related to the electron transfer rates using the Marcus theory. These reactions include electron transfer from cytochrome c_2 to the oxidized dimer, charge recombination from the primary electron acceptor quinone, and the initial forward electron transfer.

KEY WORDS: Bacterial photosynthesis; cytochrome; hydrogen bond; infrared spectroscopy; membrane protein; purple bacteria; site-directed mutagenesis.

INTRODUCTION

In photosynthesis, light energy is converted into chemical energy through a series of electron and proton transfer processes. The primary process of bacterial photosynthesis occurs in a pigment–protein complex called the reaction center (for reviews see Feher *et al.*, 1989; Parson, 1991; Kirmaier and Holten, 1993). In *Rhodobacter sphaeroides*, the reaction center consists of three subunits, L, M, and H, and a number of cofactors. The cofactors are divided into two branches, A and B, that are related by an approximate twofold symmetry axis that also relates the L and M subunits. Light excites the primary electron donor (P),[2] and an electron is transferred from the donor to an intermediate acceptor in ~3 ps. The electron is then transferred to the primary quinone Q_A in 200 ps and then to the secondary quinone acceptor Q_B in 150 μs. Cyclic electron transfer is achieved through a series of subsequent electron and proton transfer processes involving the reaction center, cytochrome bc_1 complex, and a water-soluble cytochrome c_2.

The primary electron donor, a bacteriochlorophyll *a* (Bchl) dimer, plays a critical role in the ability of the reaction centers to perform these electron transfer processes with a quantum yield of ~1. In this review we examine two specific questions concerning the donor: (1) what Bchl-protein interactions determine the energy levels of the ground state (P), the excited state (P*), and the oxidized state (P^+) of the donor, in particular focusing on the oxidation potential of the donor, and (2) what effect changes of these energy levels have on the rates of electron transfer reactions that involve the donor. This review describes how hydrogen bonding is an important determinant of the

[1] Department of Chemistry and Biochemistry, and Center for the Study of Early Events in Photosynthesis, Box 871604, Arizona State University, Tempe, Arizona 85287-1604.

[2] Abbreviations: Bchl, bacteriochlorophyll; Bphe, bacteriopheophytin; H_A, A branch bacteriopheophytin; P, bacteriochlorophyll dimer; Q_A, primary quinone; Q_B, secondary quinone.

0145-479X/95/0600-0275$07.50/0

functional properties of the donor and how the oxidation potential can be systematically altered by changing the number of hydrogen bonds formed between the donor and the surrounding amino acids.

THE PRIMARY ELECTRON DONOR

The primary electron donor in bacterial reaction centers is a Bchl dimer that is buried within the surrounding protein on the periplasmic side of the membrane (Deisenhofer *et al.*, 1984; Allen *et al.*, 1987; Chang *et al.*, 1991; Ermler *et al.*, 1994). The two halves of the dimer, designated A and B, overlap in ring I where they are separated by ~3.5 Å. The two Bchls are closely interacting, leading to an approximately equal distribution of the electrons across the entire dimer (Lubitz, 1991). Axial ligands for each Bchl are provided in *Rb. sphaeroides* by the histidine residues L173 and M202, which are conserved among bacterial reaction centers. One of the few other specific interactions between the dimer and the protein is hydrogen bonding between the Bchl and nearby amino acid residues. Structural and spectroscopic data indicate that in the wild-type *Rb. sphaeroides* reaction center, only one hydrogen bond is found, between His L168 and the acetyl group of the A-side Bchl of the dimer (Lin *et al.*, 1994a; Mattioli *et al.*, 1994). Experiments in the closely related bacterium, *Rhodobacter capsulatus*, had shown that substituting a histidine residue for a phenylalanine in the symmetry-related position near the B-side Bchl caused significant changes in the properties of the donor, including an increase in the oxidation potential (Stocker *et al.*, 1992; Taguchi *et al.*, 1992). In this review we discuss the results of altering the hydrogen bonding to the dimer in *Rb. sphaeroides*.

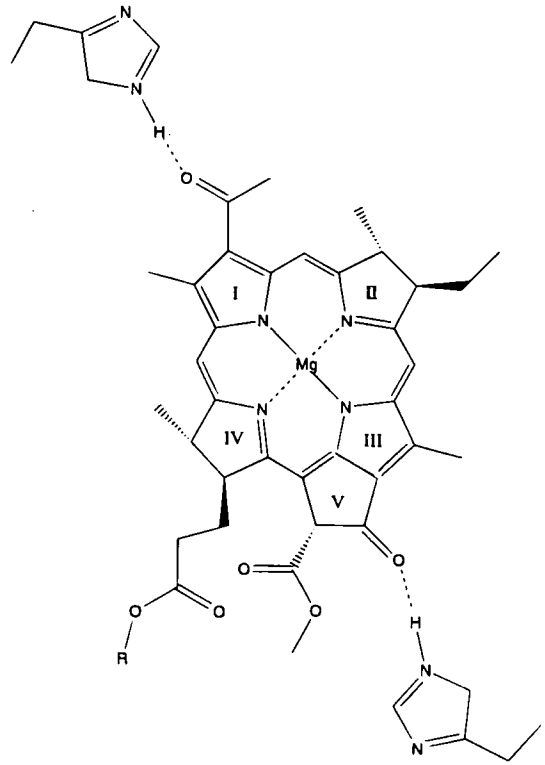

Fig. 1. Diagram of a Bchl *a* molecule which comprises one-half of the primary electron donor in the reaction center, showing positions of the two carbonyl groups that are part of the conjugated pathway and involved in hydrogen bonds. Also shown are histidine residues forming hydrogen bonds to the ring I, 2-acetyl group and the ring V, 9-keto group. In the wild-type reaction centers, only one hydrogen bond is found, between histidine L168 and the 2-acetyl group of the A-side Bchl of the donor. In the mutants, histidines are present that could form additional hydrogen bonds. When a histidine is introduced at residue M197, a hydrogen bond is made to the 2-acetyl group of the B-side Bchl of the dimer, and when histidines are introduced at residues L131 and M160, hydrogen bonds are formed with the 9-keto groups of the A-side and B-side Bchls, respectively. R represents the phytyl chain.

ALTERATION OF HYDROGEN BONDING TO THE PRIMARY ELECTRON DONOR

For each Bchl there are two groups, the 9-keto group of ring V and the 2-acetyl group of ring I, which are part of the conjugated π electronic system and are possible proton acceptors for hydrogen bonds (Fig. 1). To characterize the effects of alterations in the hydrogen bonding patterns on the oxidation potential of the dimer, mutants in *Rb. sphaeroides* have been constructed with changes near each of the four conjugated carbonyl positions. For the 2-acetyl positions, the mutation histidine to phenylalanine at L168, which breaks the hydrogen bond present on the A-side Bchl in wild type, was made in the mutant HF(L168) and the mutation phenylalanine to histidine at the symmetry-related position at residue M197 was made in the mutant FH(M197) (Murchison *et al.*, 1993; Lin *et al.*, 1994a). For both of the 9-keto positions, modeling showed that a histidine could be placed in a position favorable for the formation of a hydrogen bond without any steric hindrance with nearby amino acid residues (Williams *et al.*, 1992). These individual mutants are LH(L131), designed to add a hydrogen bond to the 9-keto group of the A-side Bchl by replacing leucine with histidine at residue L131, and LH(M160), designed to add a hydrogen bond to the 9-keto group of the B-

side Bchl by replacing leucine with histidine at residue M160. A series of mutants containing all of the double combinations of these individual changes was constructed, and a triple mutant incorporating the three mutations that result in addition of a hydrogen bond was also made (Lin *et al.*, 1994a). Thus, reaction centers with the donor having a range of hydrogen bond interactions, from none to all four carbonyl positions being possibly hydrogen bonded, were available (Table I).

SPECTRAL PROPERTIES OF HYDROGEN BOND MUTANTS

A number of spectroscopic techniques were used to probe the hydrogen-bonding state of the dimer, as well as to obtain information on the electron spin distribution and the general structural features of the dimer. The results are consistent with well-defined, local changes of the structure due to the alteration of hydrogen bonding. Specific changes in the hydrogen-bonding states of the dimer have been determined using near-infrared spectroscopy. Light-induced Fourier transform infrared difference spectra exhibited large frequency downshifts in the 9-keto carbonyl stretching region of the $P^+Q_A^-/PQ_A$ difference spectra in the LH(L131) and LH(M160) mutants relative to wild type (Nabedryk *et al.*, 1993). These changes observed in the infrared spectra of the mutants support the conclusion that hydrogen bonds have been introduced to the dimer at the 9-keto position, and they suggest a stronger hydrogen bond in LH(L131) than in LH(M160).

Well-resolved infrared spectra of the primary donor without the surrounding protein and cofactors were obtained by using Fourier transform Raman spectroscopy with selective excitation of the donor (Mattioli *et al.*, 1994, 1995). Downshifts were observed for the bands assigned to the carbonyl groups near each of the histidine residues introduced by mutagenesis, indicating that a hydrogen bond had been formed. An upshift of one carbonyl band was observed when the existing hydrogen bond to His L168 was removed. These experiments have provided direct evidence for the hydrogen bonding states of the conjugated carbonyls and have confirmed the designed hydrogen bonds in reaction centers with single site and multiple mutations. In addition, from the extent of the shift of the infrared transitions it is possible to estimate the strength of the hydrogen bond for each mutation.

The electronic state of P^+ in the mutants was determined using electron nuclear double resonance spectroscopy on isolated reaction centers (Rautter *et al.*, 1992). Shifts in the line positions were assigned to changes in the methyl proton hyperfine coupling constants for all of the mutants. The calculated spin densities were found to vary over a large range and

Table I. Comparison of P/P^+ Midpoint Potentials and Electron Transfer Times

Strain	Number of hydrogen bonds	P/P^+ midpoint potential (mV)[a]	ΔE_m (mV)[a]	$P^+Q_A^- \rightarrow PQ_A$ charge recombination time (ms)[a]	$P^+cyt^{2+} \rightarrow Pcyt^{3+}$ electron transfer time (ns)[b]	P* decay time (ps)[c]
HF(L168)	0	410	−95	220	7730	3.6
HF(L168)+LH(M160)	1	485	−20	110	1545	
LH(L131)+HF(L168)	1	485	−20	175	4820	
Wild type	1	505	0	100	960	3.5
HF(L168)+FH(M197)	1	545	40	55	1515	
LH(M160)	2	565	60	75	345	5.7
LH(L131)	2	585	80	70	470	12.2
FH(M197)	2	630	125	65	185	
LH(L131)+LH(M160)	3	635	130	60	210	25
LH(M160)+FH(M197)	3	700	195	45	130	
LH(L131)+FH(M197)	3	710	205	55	165	
LH(L131)+LH(M160)+FH(M197)	4	765	260	40	80	50

[a] From Lin *et al.*, (1994a). ΔE_m is the change in P/P^+ midpoint potential relative to wild type.
[b] From Lin *et al.*, (1994b). These values are the rates for the major fast component representing transfer when the cytochrome is tightly bound to the reaction center.
[c] From Williams *et al.* (1992), Murchison *et al.* (1993), Woodbury *et al.* (1994), and Woodbury *et al.* (1995).

were described in terms of a molecular orbital model. For the keto mutants, the model predicts a preferential stabilization of the Bchl side due to the introduction of a new hydrogen bond. For the acetyl mutations, the model indicates that the spin density is partially determined by an additional structural change that is probably rotation of the acetyl groups.

Optical absorption spectra of reaction centers contain absorption bands in the near infrared and visible regions that are characteristic of the Bchl and bacteriopheophytin (Bphe) cofactors. In particular, the donor has absorption band at ~865 nm due to a transition between the ground and excited state of the donor (P/P* transition). The band arises from the exciton coupling of the two Bchls and is sensitive to structural changes of the dimer (Plato *et al.*, 1991; Thompson *et al.*, 1991). In general the spectra of the mutant reaction centers were similar to wild type, indicating that the mutations probably have not caused gross structural changes (Williams *et al.*, 1992; Murchison *et al.*, 1993; Mattioli *et al.*, 1995). Although differences are evident in the bandshapes of the ~865 nm transition for some mutants, the shifts of the peak positions are small and modeling studies are consistent with the minor spectral shifts arising from the presence of the hydrogen bonds rather than structural alterations of the cofactors. The exceptions are the reaction centers that contain the mutation histidine to phenylalanine at L168, as the loss of the constraining hydrogen bond to L168 apparently results in a rotation of the acetyl group and a consequential blue shift of the optical band. Likewise in the mutants, the time-resolved fluorescence due to the excited state P* has a similar spectrum to wild type with only minor changes despite significant alterations of the rates of decay (Williams *et al.*, 1992; Murchison *et al.*, 1993). Thus, for most hydrogen bond mutants, the energy level of the excited state P* is essentially unchanged relative to the ground state P.

DEPENDENCE OF OXIDATION POTENTIAL UPON HYDROGEN BONDING

The P/P^+ midpoint potentials of the reaction centers were determined from electrochemical titrations of isolated reaction centers (Fig. 2). The loss of the existing hydrogen bond resulted in a 95 mV decrease in the midpoint potential, and the addition of each hydrogen bond resulted in a 60 to 125 mV increase in the midpoint potential (Table I). For example, the

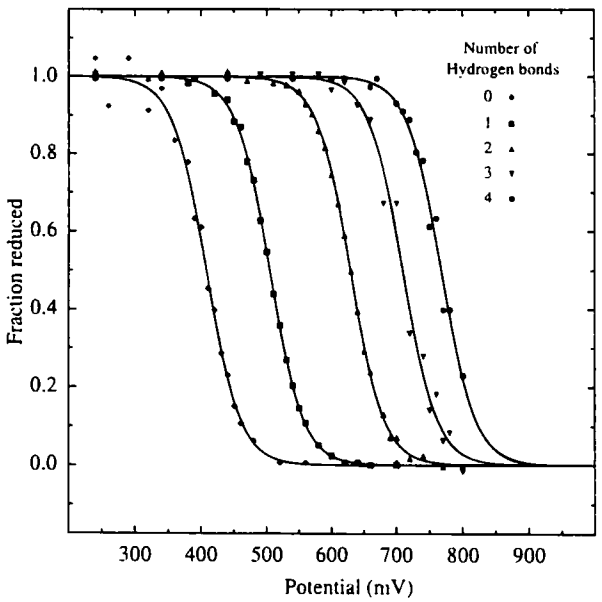

Fig. 2. Electrochemical oxidation–reduction titrations of the primary electron donor in reaction centers from wild type and several mutants of *Rb. sphaeroides*. The oxidation potential changes over a large range in response to mutations introducing histidine residues near the conjugated carbonyls of the donor. The data shown are for reaction centers from the following strains: 0 hydrogen bonds, HF(L168); 1 hydrogen bond, wild type; 2 hydrogen bonds, FH(M197); 3 hydrogen bonds, LH(L131)+FH(M197); 4 hydrogen bonds, LH(L131)+LH(M160)+FH(M197). The midpoint potentials of all the mutants are listed in Table I. Modified from Lin *et al.*, (1994a).

midpoint potential of the HF(L168)+LH(M160) mutant, in which one hydrogen bond is broken and another one is added, is nearly identical to that of wild type (only 20 mV below). Due to this additive effect, an exceptionally wide span of midpoint potentials was obtained, ranging from 410 mV, or 95 mV below wild type for the mutant with no hydrogen bonds, to a high midpoint potential of 765 mV, or 260 mV above wild type, for the mutant in which all four positions are hydrogen bonded (Table I).

The mutation phenylalanine to tyrosine at M197 also results in the addition of a hydrogen bond to the 2-acetyl group of the B-side Bchl of the dimer (Wachtveitl *et al.*, 1993b), and thus can be compared to the FH(M197) mutant that contains the mutation phenylalanine to histidine at M197. Although both mutations result in the addition of a hydrogen bond, the increase of 125 mV in the potential relative to wild type in the phenylalanine to histidine mutant is much larger than the 25 mV increase observed for the phenylalanine to tyrosine mutant. The larger change in poten-

tial for histidine compared to tyrosine is probably due to two different aspects of the mutations (see Mattioli *et al.*, 1994). First, the histidine formed a much stronger hydrogen bond than the tyrosine. In general, a correlation is observed between the potential change and the total change in hydrogen bonding strength (Mattioli *et al.*, 1995). Second, the large potential changes probably arise from electrostatic interactions of P^+, and histidine, having a larger dipole strength, would have a stronger effect than tyrosine.

The change in midpoint potential of the dimer has been determined for a variety of other mutations in the reaction center (Table II). Many of these mutations involve changes in nonspecific interactions between amino acid residues and the dimer, such as Van der Waals interactions, and do not result in large changes in the oxidation potential. Among those previously studied are mutations at tyrosine M210 that is within 5 Å of P but not in a position suitable for hydrogen bonding to P. The change of this residue to histidine resulted in a 36 mV decrease in potential (Jia *et al.*, 1993), demonstrating that the large changes in potential do not simply arise due to the introduction of histidines near the dimer, but requires the orientation of the histidine in hydrogen-bonding position. This requirement can be understood in terms of the structure of the histidine, as a hydrogen bond directly aligns the dipole moment of histidine with respect to the Bchl.

For most proteins with an electron donor, the largest changes in oxidation/reduction potential arise due to a change in the coordination of the cofactor (reviewed in Wuttke and Gray, 1993). For example, in cytochrome *c* and myoglobin it has been established the changes in the axial ligation result in potential changes of several hundred millivolts. Similarly, in the reaction center, mutation of the histidine ligand of the dimer results in a large change in the potential, which is comparable to the changes observed in the hydrogen bond mutant. When the axial histidine ligand at M202 of the B-side Bchl of the dimer is changed to leucine, the resulting mutant contains a "heterodimer," as it has a Bchl-Bphe dimer (Bylina and Youvan, 1988; McDowell *et al.*, 1991). The structure of the reaction center from the heterodimer mutant is similar to that of wild type, although there are small shifts in the relative positions of the two halves of the dimer and in the positions of nearby amino acid residues (Chirino *et al.*, 1994). The midpoint potential for Bphe is intrinsically higher than for Bchl, and causes the charge in the oxidized state to preferentially localize on the Bchl side of the heterodimer (Huber *et al.*, 1990). Thus, changing the axial ligand results in a reaction center with a different cofactor composition, and an increase of 160 mV in the midpoint potential is observed compared to wild type (Table II).

Table II. Redox Measurements on Other Mutant Reaction Centers[a]

Position	Native	Mutation	ΔE_m (mV)	Reference
L162	Tyr	Leu	50	Wachtveitl *et al.*, 1993a
		Gly	50	Wachtveitl *et al.*, 1993a
		Phe	30	Wachtveitl *et al.*, 1993a
L167	Phe	Leu	25	Murchison *et al.*, 1993
L181	Phe	Lys	7	Jia *et al.*, 1993
		Glu	−17	Jia *et al.*, 1993
		Tyr	−25	Jia *et al.*, 1993
		Thr	−26	Jia *et al.*, 1993
L244	Ser	Gly	35	Wachtveitl *et al.*, 1993b
L248	Met	Thr	0	Wachtveitl *et al.*, 1993b
M197	Phe	Tyr	25	Wachtveitl *et al.*, 1993b
M210	Tyr	Trp	52	Nagarajan *et al.*, 1993
		Ile	33	Nagarajan *et al.*, 1993
		Phe	30	Nagarajan *et al.*, 1993
			11	Jia *et al.*, 1993
		Thr	16	Jia *et al.*, 1993
		His	−36	Jia *et al.*, 1993
L181/M210	Phe/Tyr	Thr/Thr	25	Jia *et al.*, 1993
		Tyr/Phe	−5	Jia *et al.*, 1993
		His/His	−55	Jia *et al.*, 1993
M202	His Bchl/Bchl	Leu Bchl/Bphe	160	Davis *et al.*, 1992

[a] Measurements are for reactions centers from *Rb. sphaeroides* except for the values from Jia *et al.* (1993) that are based upon reaction centers from *Rb. capsulatus*. The residue numbering is for *Rb. sphaeroides;* the residue equivalent to tyrosine M210 in *Rb. sphaeroides* is tyrosine M208 in *Rb. capsulatus*. ΔE_m is the change in the P/P^+ midpoint potential compared to wild type.

ELECTRON TRANSFER RATES

The changes in the P/P^+ midpoint potential in the mutants are assumed to cause parallel changes in the energy levels of each of the charge separated states,

thus altering the driving force, $\Delta G°$, for several electron-transfer reactions (Fig. 3). For example, an increase in the P/P^+ midpoint potential leads to a decrease in the driving force for the initial electron transfer but an increase in the driving force for charge recombination. The effect of changes in $\Delta G°$ on electron transfer rates has been modeled for biological systems (as discussed in several other articles in this issue). In the Marcus model that assumes that the donor and the acceptor are coupled to a single vibrational mode in a harmonic approximation (Jortner, 1976), the rate is given by

$$k\alpha\left(\frac{\nu + 1}{\nu}\right)^{p/2} \exp[-S(2\nu + 1)]I_p(2S\sqrt{\nu(\nu + 1)}) \quad (1)$$

where $\nu = 1/[\exp(h\nu/k_BT) - 1]$, which is the thermal population of a mode with vibrational frequency ν at temperature T, k_B is the Bolzmann constant, $p = -\Delta G°/h\nu$, $I_p()$ is a modified Bessel function of order p, and $S = \lambda/h\nu$, where λ is the reorganization energy (Marcus and Sutin, 1985). In the high-temperature limit where $h\nu << k_BT$, this reduces to the classical expression

$$k\alpha\ (4\pi\lambda k_BT)^{-1/2} \exp\ [-(\Delta G° + \lambda)^2/(4\lambda k_BT)] \quad (2)$$

Experimental measurements of the electron transfer rates in the mutants have been analyzed using these models. The rates for three processes, electron transfer from cytochrome c_2, charge recombination from the primary quinone, and the initial forward electron transfer have been measured in the hydrogen bond mutants (Table I). These processes span a wide range of time scales, from picoseconds to milliseconds, and are modeled using these two relationships as described below.

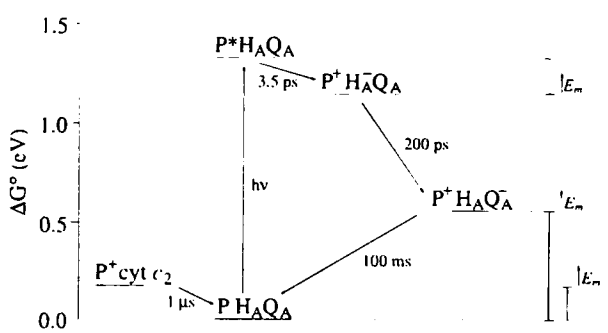

Fig. 3. Simplified free-energy diagram of the energy levels of the cofactors of the reaction center, and of cytochrome c_2, which is the secondary electron donor. An increase in the P/P^+ midpoint potential, E_m, such as is found in the hydrogen-bond mutants, will affect the free-energy difference for several electron-transfer reactions.

Electron Transfer from Cytochrome c_2

In order to achieve cyclic electron transfer, a water-soluble cytochrome c_2 must bind to the reaction center and donate an electron to the oxidized donor (reviewed in Tiede and Dutton, 1993). After transfer the oxidized cytochrome leaves and is replaced by another cytochrome. For electron transfer from the cytochrome to the reaction center the free-energy difference between the initial state, P^+ cyt^{2+}, and the final state, P cyt^{3+}, is determined by the relative difference in the oxidation/reduction midpoint potentials of P and cytochrome c_2. For the hydrogen-bond mutants, the alteration of the P/P^+ midpoint potential results in a range of $\Delta G°$ from 65 to 420 meV compared to 160 meV for wild type. The electron-transfer rates were measured in isolated reaction centers with exogenous cytochrome c_2. As the driving force becomes larger, the characteristic times decrease over several orders of magnitude, from 7730 to 80 ns for the mutants compared to 960 ns for wild type (Table I). Other properties of the reaction, such as the binding of the cytochrome to the reaction center, were essentially unchanged in the mutants. The data are well fit to Eq. (2) using a value of λ equal to ~500 meV (Fig. 4A). The estimated value of the reorganization energy is consistent with values of ~800 meV for the reorganization energy in cytochrome b_5 determined from cytochrome-ruthenium experiments (Jacobs *et al.*, 1991) and metal-substitution experiments involving cytochrome b_5 and cytochrome c (McLendon, 1988).

Although the data do not reach to the inverted region, the fit of the cytochrome electron transfer data predicts a maximal rate of 1.4×10^7 s^{-1} when the free-energy difference equals the reorganization energy. According to the model of Moser *et al.* (1992) this maximal rate can be used to empirically predict the edge-to-edge distance between the heme and the bacteriochlorophyll dimer to be ~14 Å. Alternatively, using the model of Beratan *et al.* (1992), a smaller edge-to-edge distance of ~9 Å is estimated. Thus, the predicted distances range from 9 to 14 Å, which is in general agreement with distances derived from modeling studies of the reaction center–cytochrome complex (Allen *et al.*, 1987; Tiede and Chang, 1988).

Charge Recombination

In wild-type reaction centers the electron is transferred from Q_A^- to Q_B in ~150 μs and so charge

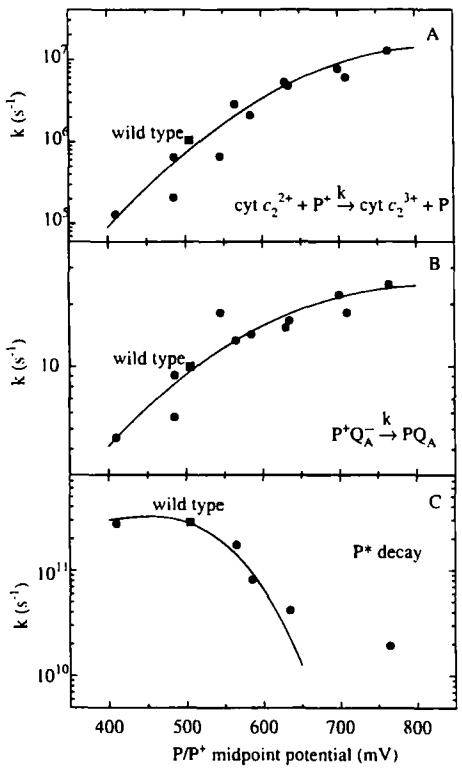

Fig. 4. The relationship between the P/P+ midpoint potential and electron-transfer rate for (A) electron transfer from cytochrome c_2 to the oxidized dimer, (B) charge recombination from the primary quinone, and (C) P* decay, which is indicative of the initial charge separation. The data are shown in Table I and are fit using: (A) Eq. (2) with λ = 500 meV, (B) Eq. (1) with λ = 900 meV and ν = 1240 cm^{-1}, and (C) Eq. (1) modified with two different modes having frequencies of 95 and 1500 cm^{-1}, reorganization energies of 800 cm^{-1}, and a value of -480 cm^{-1} for ΔG° in wild type as described in Bixon *et al.* (1995). This fit was based upon mutants with midpoint potentials less than 600 meV. Panels A and B are modified from Lin *et al.* (1994a,b).

recombination from Q_A^-, which has a time constant of ~100 ms, normally does not occur. However, the charge recombination process in isolated reaction centers can be studied by either biochemically removing the secondary quinone or by blocking electron transfer to Q_B with an inhibitor. The driving force for the charge recombination reaction is determined by the difference in the P/P+ and Q/Q− midpoint potentials, and since the Q/Q− potential is small, the free-energy difference for the wild type is ~500 meV. For the mutants the value of the recombination time from the primary quinone was found to vary from 220 to 40 ms compared to 100 ms for wild type (Table I). The data are well fit to Eq. (1) when the parameters were adjusted to the values λ = 900 meV and ν = 1240 cm^{-1} (Fig. 4B). The fit required a high frequency of the vibrational mode, necessitating the use of the more general relation rather than the classical expression. Such modes are probably associated with the quinone, and the possible contribution of additional vibrational modes cannot be determined from these data since a maximum rate has not been clearly observed. The relationship between the charge recombination rate and driving force has been studied previously by altering the driving force either by the application of electric fields or by replacing the native ubiquinone with quinones with other redox potentials (Gunner *et al.*, 1986; Popovic *et al.*, 1986; Feher *et al.*, 1988; Franzen and Boxer, 1993). In general, the results on the hydrogen bond mutants are consistent with the previous measurements. The estimated value of 900 meV for the reorganization energy at 295 K is ~200 meV higher than the value previously estimated based upon experiments at low temperatures (below 100 K). This suggests that the reorganization energy becomes lower with temperature, as has been also noted by others (Franzen and Boxer, 1993; Dutton and Moser, 1994).

Initial Electron Transfer

Within ~3 ps after excitation of the donor to the singlet excited state P*, an electron is transferred to the bacteriopheophytin H_A (reviewed in Kirmaier and Holten, 1993; Parson, 1991). This reaction is generally measured by the rate of decay of the stimulated emission of the excited state P*. Femtosecond transient absorption measurements on several mutants show that the rate of the decay of P* clearly becomes slower for the mutants that have larger midpoint potentials, although a complete set of data on the entire series of hydrogen-bond mutants has not been taken (Table I). This is consistent with the driving force decreasing in those mutants with an increased midpoint potential and thus leading to a decrease in rate.

Modeling of this process is difficult due to several factors. The free-energy difference cannot be calculated directly since the H_A/H_A^- potential cannot be measured, although indirect measurements have estimated the $P^*/P^+H_A^-$ energy difference to be approximately 100–200 meV (reviewed in Peloquin *et al.*, 1994; Woodbury *et al.*, 1994). One of the monomer Bchls may serve as an electron acceptor prior to transfer to H_A; however, experimental characterization of the properties of the monomer Bchl is difficult (Holzapfel *et al.*, 1989; Kirmaier and Holten, 1991). In

addition, the assignment of rate constants, which is necessary for the modeling, is difficult due to multiexponential decays of the measured absorption and emission changes (Woodbury and Allen, 1994).

A general model based upon Eq. (1) has been developed to incorporate these factors as parameters (Bixon *et al.*, 1995). A fit of mutants with various changes in the P/P^+ midpoint potential was reported using both low-frequency (95 cm^{-1}) and high-frequency (1500 cm^{-1}) modes (Fig. 4C). The mutant HF(L168) should have a larger driving force than wild type, and an initial study showed that the rate at room temperature was similar to wild type (Murchison *et al.*, 1993). Further analysis of this mutant at different temperatures may reveal new features, such as a definite role for the Bchl monomer. Some results for mutants with high midpoint potentials, such as the triple mutant LH(L131)+LH(M160)+FH(M197), indicate that a simple Marcus model may not adequately describe the initial electron transfer. For example, in the triple mutant the state $P^+H_A^-$ should be energetically above P* and thus be thermodynamically unfavorable; however, the initial electron transfer still takes place, even at low (20 K) temperatures (Woodbury *et al.*, 1995). These experimental data are not consistent with the fit to the Marcus model, which predicts a characteristic time of slower than 1000 ps at room temperature (Fig. 4C), suggesting that electron transfer may be proceeding by a different mechanism in the triple mutant than dominates for wild type (Bixon *et al.*, 1995). In general, the mutants provide a system for quantitatively evaluating models in which λ and ΔG° are not well defined and change with temperature or time (Bixon *et al.*, 1995; Woodbury *et al.*, 1994, 1995).

CONCLUSIONS

The characterization of reaction-center mutants has provided the opportunity to determine what interactions between an electron donor and nearby amino acids determine the energy levels of the donor. Changes in interactions that are nonspecific, such as Van der Waals interactions, result in only small changes in potential. A large change in the potential does arise when a Bchl ligand is changed, but associated with this mutant is a significant change in composition. In contrast, it is possible to engineer other interactions, namely hydrogen-bond interactions, that lead to successive increases in the midpoint potential of an electron donor without significantly altering the structure. Thus, nonligand interactions can play a significant role in establishing the oxidation potential of a donor. To quantitatively model the interactions that give rise to these potential changes, characterization of mutants with a variety of different amino acid residues at the hydrogen bonding sites is planned. The identification of interactions that lead to large changes in potential may explain how the midpoint potentials of chlorophyll cofactors in a variety of photosynthetic proteins, from bacterial reaction centers to photosystem II, can vary by several hundred millivolts.

These studies allow the characterization of the relationship between the rate and driving force for both interprotein and intraprotein electron transfer with a fixed donor–acceptor distance. The results show that a variation in the rate up to two orders of magnitude can be achieved by a 350-meV range of free-energy differences. The specific properties of each electron-transfer reaction studied are clearly different; for example, the value of the reorganization energy ranges from approximately 100 meV for the initial charge separation to 900 meV for charge recombination from the primary quinone. In general, the change in the electron-transfer rates for the initial charge separation and the electron transfer from the cytochrome was much greater than the change in the charge-recombination rate for a given change in the oxidation potential of the dimer. The variation in the parameters for each reaction probably reflects the individual requirements for times and distances, as well as differences in the nature of the cofactors involved in each transfer step (Moser *et al.*, 1992). The factors governing the electron-transfer processes will be further elucidated by measuring the rates as a function of temperature for the mutants.

The rate versus driving force relationship has been studied within a protein complex in photosynthetic systems primarily for charge recombination. Studies of interprotein electron transfer in nonphotosynthetic systems are limited, as they involve alteration of the protein by metal substitution or covalent attachment of redox active groups (for a review, see McLendon, 1988). The results on the hydrogen-bond mutants provide estimates for electron-transfer parameters such as the reorganization energy that should be applicable to other biological systems, especially those involving cytochromes, which are commonly found as electron carriers, and other photosystems.

ACKNOWLEDGMENTS

We are grateful for the contributions of our collaborators, including the research groups of J. Breton, W. Lubitz, P. Mathis, T. Mattioli, W. Parson, and N. Woodbury. The work described in this review was supported by grants from the National Institutes of Health (GM45902) and the National Science Foundation (MCB-9404925). This is publication No. 242 from the Arizona State University Center for the Study of Early Events in Photosynthesis.

REFERENCES

Allen, J. P., Feher, G., Yeates, T. O., Komiya, H., and Rees, D. C. (1987). *Proc. Natl. Acad. Sci. USA* **84**, 6162–6166.

Beratan, D. N., Onuchic, J. N., Winkler, J. R., and Gray, H. B. (1992). *Science* **258**, 1740–1742.

Bixon, M., Jortner, J., and Michel-Beyerle, M. E. (1995). *Chem. Phys.* **197**.

Bylina, E. J., and Youvan, D. C. (1988). *Proc. Natl. Acad. Sci. USA* **85**, 7226–7230.

Chang, C.-H., El-Kabbani, O., Tiede, D., Norris, J., and Schiffer, M. (1991). *Biochemistry* **30**, 5352–5360.

Chirino, A. J., Lous, E. J., Huber, M., Allen, J. P., Schenck, C. C., Paddock, M. L., Feher, G., and Rees, D. C. (1994). *Biochemistry* **33**, 4584–4593.

Davis, D., Dong, A., Caughey, W. S., and Schenck, C. C. (1992). *Biophys. J.* **61**, A153.

Deisenhofer, J., Epp, O., Miki, K., Huber, R., and Michel, H. (1985). *Nature (London)* **318**, 618–624.

Dutton, P. L., and Moser, C. C. (1994). *Proc. Natl. Acad. USA* **91**, 10247–10250.

Ermler, U., Fritzsch, G., Buchanan, S. K., and Michel, H. (1994). *Structure* **2**, 925–936.

Feher, G., Arno, T. R., and Okamura, M. Y. (1988). In *The Photosynthetic Bacterial Reaction Center* (Breton, J., and Verméglio, A., eds.), Plenum, New York, pp. 271–287.

Feher, G., Allen, J. P., Okamura, M. Y., and Rees, D. C. (1989). *Nature (London)* **339**, 111–116.

Franzen, S., and Boxer, S. G. (1993). *J. Phys. Chem.* **97**, 6304–6318.

Gunner, M. R., Robertson, D. E., and Dutton, P. L. (1986). *J. Phys. Chem.* **90**, 3783–3795.

Holzapfel, W., Finkele, V., Kaiser, W., Oesterhelt, D., Scheer, H., Stilz, H. U., and Zinth, W. (1989). *Chem. Phys. Lett.* **160**, 1–7.

Huber, M., Lous, E. J., Isaacson, R. A., Feher, G., Gaul, D., and Schenck, C. C. (1990). In *Reaction Centers of Photosynthetic Bacteria* (Michel-Beyerle, M. E., ed.), Springer Verlag, Berlin, pp. 219–228.

Jacobs, B. A., Mauk, M. R., Funk, W. D., MacGillivray, R. T. A., Mauk, A. G., and Gray, H. B. (1991). *J. Am. Chem. Soc.* **113**, 4390–4394.

Jia, Y., DiMagno, T. J., Chan, C-K., Wang, Z., Du, M., Hanson, D. K., Schiffer, M., Norris, J. R., Fleming, G. R., and Popov, M. S. (1993). *J. Phys. Chem.* **97**, 13180–13191.

Jortner, J. (1976). *J. Chem. Phys.* **64**, 4860–4867.

Kirmaier, C., and Holten, D. (1991). *Biochemistry* **30**, 609–613.

Kirmaier, C., and Holten, D. (1993). In *The Photosynthetic Reaction Center*, Vol. II (Deisenhofer, J., and Norris, J. R., eds.), Academic Press, San Diego, pp. 49–70.

Lin, X., Murchison, H. A., Nagarajan, V., Parson, W. W., Allen, J. P., and Williams, J. C. (1994a). *Proc. Natl. Acad. Sci. USA* **91**, 10265–10269.

Lin, X., Williams, J. C., Allen, J. P., and Mathis, P. (1994b). *Biochemistry* **33**, 13517–13523.

Lubitz, W. (1991). In *Chlorophylls* (Scheer, H. ed.), CRC Press, Boca Raton, pp. 903–944.

Marcus, R. A., and Sutin, N. (1985). *Biochim. Biophys. Acta* **811**, 265–322.

Mattioli, T. A., Williams, J. C., Allen, J. P., and Robert, B. (1994). *Biochemistry* **33**, 1636–1643.

Mattioli, T. A., Lin, X., Allen, J. P., and Williams, J. C. (1995). *Biochemistry* **34**, 6142–6152.

McDowell, L. M., Gaul, D., Kirmaier, C., Holten, D., and Schenck, C. C. (1991). *Biochemistry* **30**, 8315–8322.

McLendon, G. (1988). *Acc. Chem. Res.* **21**, 160–167.

Moser, C. C., Keske, J. M., Warncke, K., Farid, R. S., and Dutton, P. L. (1992). *Nature (London)* **355**, 796–802.

Murchison, H. A., Alden, R. G., Allen, J. P., Peloquin, J. M., Taguchi, A. K. W., Woodbury, N. W., and Williams, J. C. (1993). *Biochemistry* **32**, 3498–3505.

Nagarajan, V., Parson, W. W., Davis, D., and Schenck C. C. (1993). *Biochemistry* **32**, 12324–12336.

Nabedryk, E., Allen, J. P., Taguchi, A. K. W., Williams, J. C., Woodbury, N. W., and Breton, J. (1993). *Biochemistry* **32**, 13879–13885.

Parson, W. W. (1991). In *Chlorophylls* (Scheer, H., ed.), CRC Press, Boca Raton, pp. 1153–1180.

Peloquin, J. M., Williams, J. C., Lin, X., Alden, R. G., Taguchi, A. K. W., Allen, J. P., and Woodbury, N. W. (1994) *Biochemistry* **33**, 8089–8100.

Plato M., Mobius, K., and Lubitz, W. (1991). In *Chlorophylls* (Scheer, H., ed.), CRC Press, Boca Raton, pp. 1015–1046.

Popovic, Z. D., Kovacs, G. J., Vincett, P. S., Alegria, G., and Dutton, P. L. (1986). *Chem. Phys.* **110**, 227–237.

Rautter, J., Gessner, C., Lendzian, F., Lubitz, W., Williams, J. C., Murchison, H. A., Wang, S., Woodbury, N. W., and Allen, J. P. (1992). In *The Photosynthetic Bacterial Reaction Center II, Structure: Spectroscopy, and Dynamics* (Breton, J., and Verméglio, A., eds.), Plenum, New York, pp. 99–108.

Stocker, J. W., Taguchi, A. K. W., Murchison, H. A., Woodbury, N. W., and Boxer, S. G. (1992). *Biochemistry* **31**, 10356–10362.

Taguchi, A. K. W., Stocker, J. W., Alden, R. G., Causgrove, T. P., Peloquin, J. M., Boxer, S. G., and Woodbury, N. W. (1992). *Biochemistry* **31**, 10345–10355.

Thompson, M. A., Zerner, M. C., and Fajer, J. (1991). *J. Phys. Chem.* **95**, 5693–5700.

Tiede, D. M., and Chang, C. H. (1988). *Isr. J. Chem.* **28**, 183–191.

Tiede, D. M., and Dutton, P. L. (1993). In *The Photosynthetic Reaction Center*, Vol. I (Deisenhofer, J., and Norris, J. R., eds.), Academic Press, San Diego, pp. 257–288.

Wachtveitl, J., Farchaus, J. W., Mathis, P., and Oesterhelt, D. (1993a). *Biochemistry* **32**, 10894–10904.

Wachtveitl, J., Farchaus, J. W., Das, R., Lutz, M., Robert, B., and Mattioli, T. A. (1993b). *Biochemistry* **32**, 12875–12886.

Williams, J. C., Alden, R. G., Murchison, H. A., Peloquin, J. M., Woodbury, N. W., and Allen, J. P. (1992). *Biochemistry* **31**, 11029–11037.

Woodbury, N. W., and Allen, J. P. (1994). In *Anoxygenic Photosynthetic Bacteria* (Blankenship, R. E., Madigan, M. T., and Bauer, C. E., eds.), Kluwer, Dordrecht, 527–557.

Woodbury, N. W., Peloquin, J. M., Alden, R. G., Lin, X., Lin, S., Taguchi, A. K. W., Williams, J. C., and Allen, J. P. (1994). *Biochemistry* **33**, 8101–8112.

Woodbury, N. W., Lin, S., Lin, X., Peloquin, J. M., Taguchi, A. K. W., Williams, J. C., and Allen, J. P. (1995). *Chem. Phys.* **197**.

Wuttke, D. S., and Gray, H. B. (1993). *Curr. Opinion Struct. Biol.* **3**, 555–563.